

EFFECT OF PREPARATION TEMPERATURE AND IONS DOPING ON SIZE, MORPHOLOGY AND CATALYTIC ACTIVITY OF Co-B AMORPHOUS NANO CATALYST

Mohammad Hassan Loghmani* and Abdollah Fallah Shojaei*

Department of Chemistry, Faculty of Science, University of Guilan, P.O. Box 1914, Rasht, Iran

(Received June 27, 2014; revised December 2, 2014)

ABSTRACT. Binary and quaternary amorphous nano powders are prepared by wet reduction method. Cobalt boride nano catalyst is synthesized at 10 and 60 °C. Effect of preparation temperature on size and morphology was studied. Co-M-Zr-B (M: Cr, Mo and W) as quaternary catalysts are also prepared in order to studying ions doping on chemical and physical properties. Indeed, the obtained materials are characterized by XRD, FE-SEM, TEM, BET and ICP techniques. No distinct peak could be observed in XRD patterns indicating that the all catalysts possessed amorphous. The catalytic activity of the synthesized catalysts is investigated for the reduction reaction of 4-nitrophenol to 4-aminophenol in the presence of excess NaBH₄ in aqueous medium at room temperature (298 K). It is found that our catalysts are highly active for high concentrations of 4-NP, 25-200 ppm.

KEY WORDS: Amorphous, Nano catalyst, Metal boride, Reduction, Nitrophenol

INTRODUCTION

In the past two decades, nanotechnology has been developed quickly in various fields. Nanoparticles have potential applications in chemistry, physics, electronics, biology, and medicine due to their unique characteristics different from bulk materials. Metal nanoparticles have been attracting great attention because of their remarkable catalytic performance in hydrogenation, oxidation, and reduction reactions [1-3]. For example, transition metal nano clusters have been studied as catalysts in various organic and inorganic reactions [4]. The catalytic activities of metal nanoparticles are strongly dependent on their sizes and shapes [5-10]. Amorphous Cobalt boride (Co-B) catalysts, prepared by reduction of metal salts with a reducing agent, have attracted great attention in catalysis owing to their unique properties such as isotropic structure, high concentration of coordinative unsaturated sites, relevant chemical stability, and low cost. However, the exothermic nature of the reduction reaction involves high surface energy causing metal-boride particles to agglomerate. This particle agglomeration lowers the effective surface area of the catalyst powder thus limiting its catalytic activity. It is found that, chemical reduction reaction is most frequently used in preparing Co-B amorphous alloys [11-15]; however, the regular Co-B samples obtained via direct reduction of cobalt salt solution with a sodium borohydride solution usually display low surface area, broadly distributed particle size, and poor thermal stability against crystallization due to aggregation, because the reduction reaction is vigorous and exothermic [16, 17]. Nitro compounds are widely generated as by-products in different industries like agrochemicals, coloring agents, and pharmaceutical products. Among various nitro compounds, 4-nitrophenol (4-NP) is one of the frequently occurring by-products, which is toxic to the environment. In pharmaceutical industries, the 4-aminophenol (4-AP) is derived from the 4-NP by reduction. The 4-AP is a vital precursor for the production of different medicines like paracetamol, phenacetin, acetanilide, etc. The reduction of 4-NP to 4-AP is a model reaction which has been widely used for the quantification and comparison of the catalytic activity of metal nanoparticles [18]. Direct hydrogenation of 4-NP catalyzed by Pt, Pd and Ru is employed for the production of 4-AP [19, 20]. However, such kind of catalysts seems to be not suitable for the industrial application

*Corresponding author. E-mail: chemlogh@gmail.com, shoja47@gmail.com

considering their cost and availability. There are a variety of methods, which can be used to convert aromatic nitro compounds to their corresponding amines. Some of them include NbCl_5/In [21], Cu [22], $\text{Ag}@/\text{SBA-15}$ [23], Au/PMMA [24] and Ag-MCM-41 [25]. In continuation of our study on oxidation of alcohols [26], photodegradation of 4-NP [27] methyl orange and methylene blue [28] we tried to reduce of 4-NP over metal boride nano catalysts. Also, previously we have synthesized Co-La-Zr-B quaternary amorphous nano alloy [29], PVP stabilized crystalline phase of Co-La-Zr-B [30] and oleic acid stabilized Co-La-Zr-B [31] for hydrogen generation through hydrolysis of sodium borohydride. In this work, two sets of catalysts, binary and quaternary amorphous powders, were prepared. First, Co-B nano catalyst was synthesized at different temperatures, 10 and 60 °C. Indeed, effect of preparation temperature on size, morphology and consequently catalytic activity of Co-B amorphous nano catalysts were studied. The second type of prepared catalysts is Co-M-Zr-B (M: Cr, Mo and W) as quaternary catalysts. The obtained materials were characterized by X-ray diffraction (XRD), field emission scanning electron microscope (FE-SEM), transmission electron microscopy (TEM), Brunauer-Emmett-Teller (BET) and inductively coupled plasma (ICP) techniques. Conversion of 4-NP to 4-AP is carried out using sodium borohydride in aqueous medium at room temperature. The reaction was monitored in a UV-Vis spectroscopy. Determination of metal leaching was done by ICP emission spectroscopy.

EXPERIMENTAL

Synthesis of Co-B binary amorphous nano catalysts

Co-B amorphous nano catalysts were prepared under Ar atmosphere. In the typical synthesis, in 250 mL three-necked round bottom flask, 952 mg (4 mmol) of $\text{CoCl}_2 \cdot 6\text{H}_2\text{O}$ was dissolved in deionized water. Color of solution is purple at this moment. Then, the mixture was purged by pure Ar to remove oxygen molecules. Under sonication 10 mL of alkaline (170 mg NaOH) sodium borohydride solution (12 mmol = 456 mg) was added drop by drop into the solution. By addition of NaBH_4 solution, abrupt color change from purple to black indicates that the formation of metal nano particles was completed. Synthesis of Co-B was accomplished at 10 and 60 °C. Obtained powders are marked as Co-B10 and Co-B60. After 15 min sonication, the fine black precipitate which was subsequently formed in the mixed solution, was filtrated out through vacuum-assisted filtration and washed repeatedly in distilled water. Then it was washed further with acetone, and dried at room temperature.

Synthesis of Co-M-Zr-B (M: Cr, Mo and W) quaternary amorphous nano catalysts

Co-M-Zr-B (M: Cr, Mo and W) amorphous nano catalysts were prepared under Ar atmosphere. In the typical synthesis, in 250 mL three-necked round bottom flask, 238 mg (1 mmol) of $\text{CoCl}_2 \cdot 6\text{H}_2\text{O}$, 266 mg (1 mmol) of $\text{CrCl}_3 \cdot 6\text{H}_2\text{O}$ or 1235 mg (1 mmol) of $(\text{NH}_4)_6\text{Mo}_7\text{O}_{24} \cdot 4\text{H}_2\text{O}$ or 337 mg (1 mmol) of $\text{Na}_2\text{WO}_4 \cdot 2\text{H}_2\text{O}$ and 233 mg (1 mmol) of ZrCl_4 were dissolved in deionized water. Then, the mixture was purged by pure Ar to remove oxygen molecules. Under sonication 5 mL of sodium borohydride solution (10 mmol = 380 mg NaBH_4 in deionized water) was added drop by drop into metals solution. By addition of NaBH_4 solution, abrupt color change was done indicates that the formation of metal nano particles was completed. The fine precipitates, which were subsequently formed in the mixed solution, was filtrated out through vacuum-assisted filtration and washed repeatedly in distilled water. Then it was washed further with acetone, and dried at room temperature. CrZ, MZ and WZ were used as abbreviation for Co-Cr-Zr-B, Co-Mo-Zr-B and Co-W-Zr-B, respectively.

Reduction process

A typical catalysis experiment was carried as follows: catalyst (6 mg), NaBH₄ aqueous solution (0.1 mL, 0.15 and 0.3 M) and 4-NP (3 mL, 25-200 ppm) were mixed together in a 10 mm path-length quartz cuvette at room temperature. The yellow color of solution gradually vanished, indicating the reduction of 4-NP. The concentration of 4-NP was determined spectrophotometrically at a wavelength of 400 nm using a RAYLEIGH UV-1800 spectrophotometer.

Characterization methods

XRD patterns were recorded by a D8 Bruker Advanced, X-ray diffractometer using Cu K α radiation ($\alpha = 1.54 \text{ \AA}$). The patterns were collected in the range of 20-70° 2 θ and continuous scan mode. SEM images were obtained on Tescan Vega II and FE-SEM Hitachi S-4160 microscopes. TEM image was obtained on a Philips CM10 transmission electron microscope with an accelerating voltage of 100 kV. The metal contents of the samples were determined by ICP-OES (Inductively Coupled Plasma Optical Emission Spectroscopy, Leeman-Direct Reading Echelle). Specific surface areas of catalysts were measured by the BET method analysis under N₂ adsorptive (SIBATA SA 1100) after degassing. The reduction product was further identified by FT-IR using a Shimadzu FTIR 470 spectrophotometer. ¹H NMR spectrum was measured on a Bruker DRX-500 Avance spectrometer.

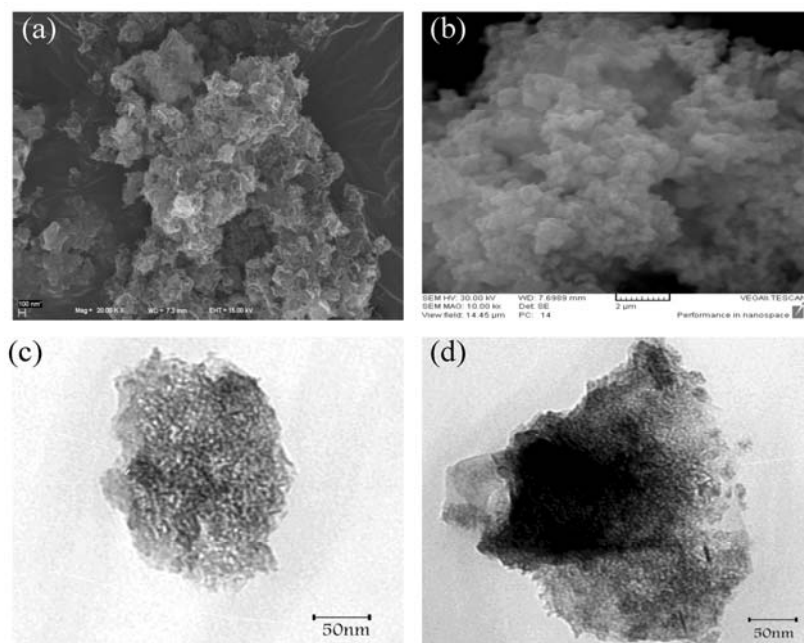
RESULTS AND DISCUSSIONS

Figure 1. SEM images of (a) Co-B10, (b) Co-B60 and TEM micrographs of (c) Co-B10 and (d) Co-B60.

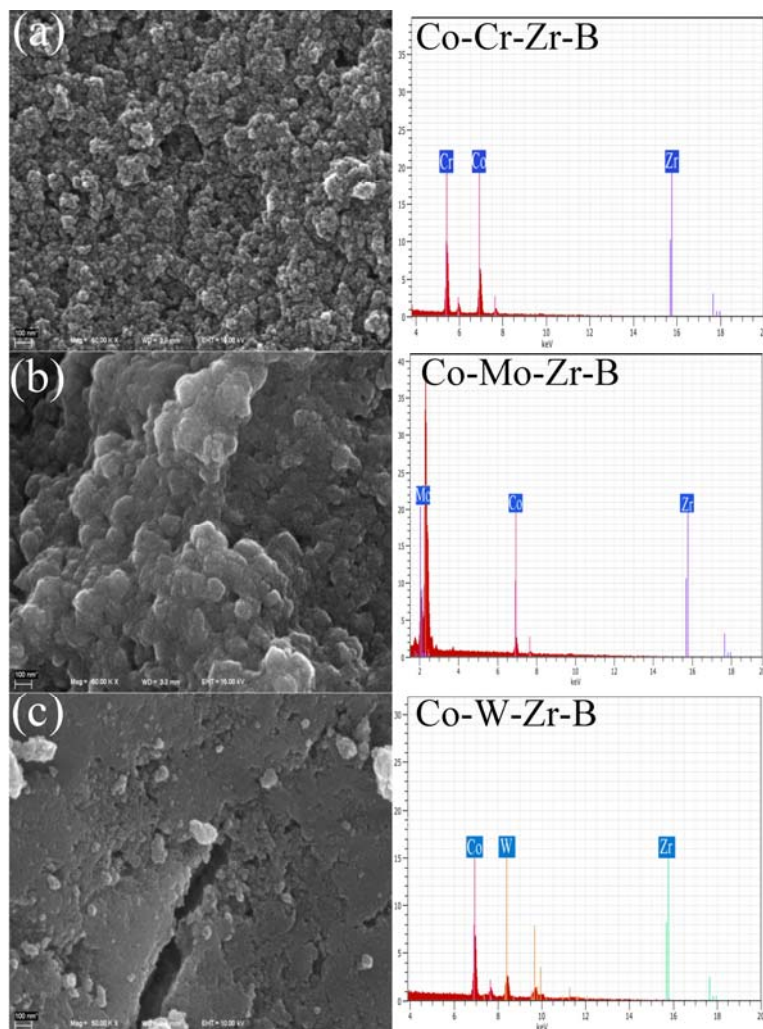


Figure 2. SEM images of (a) Co-Cr-Zr-B, (b) Co-Mo-Zr-B and (c) Co-W-Zr-B powders.

Characterization

XRD patterns of all catalysts were prepared and no distinct peak could be observed in XRD patterns (not shown) indicating that the all catalysts possessed amorphous phase. On the other hand, there is no any peak of Co_3O_4 , Cr_2O_3 , ZrO_2 , MoO_3 , WO_3 and B_2O_3 in XRD pattern indicating formation of metal oxide is inhibited under Ar atmosphere. For determination size and morphology of obtained catalysts, TEM and SEM micrographs were recorded and results are shown in Figure 1 and Figure 2. SEM images of Co-B10 and Co-B60 amorphous nano catalysts are shown in Figure 1 (a) and (b), respectively. As seen, when temperature preparation is changed from 10 to 60 °C morphology of particles has been changed. Figure 1 (a) shows that

Co-B10 is puffy form with several sheets while Figure 1 (b) shows that Co-B60 is appeared pseudo spherical and agglomerated particles. TEM micrographs of Co-B10 and Co-B60 are shown in Figure 1 (c) and (d), respectively. TEM micrographs also confirm with increasing temperature size and morphology of particles are changed. This suggests that some aggregation of Co-B nanoparticles occurs at a higher temperature.

As clearly seen, Figure 2 (a) and (c) confirm that there are no agglomerated CrZ and WZ nano particles. On the other hand, Figure 2 (b) shows that MZ particle is agglomerated. All samples show similar particle-like morphology with particles having spherical shape and size of a few nanometers. EDS pattern of each catalyst is also shown in Figure 2. The peaks around 6.95, 5.44, 2.03, 8.44 and 15.78 keV are corresponded to Co, Cr, Mo, W and Zr, respectively. As seen, intensities of all metal peaks approximately are same indicating high degree of homogeneity of powders is achieved by this method. The specific surface areas and elemental analysis of catalysts are shown in Table 1.

Table 1. Surface area and elemental analysis of catalysts

Catalyst	BET (m ² /g)	EDS ^a	ICP
Co-B 10	92	-	-
Co-B 60	61	-	-
CrZ	155	Co/Cr: 0.8, Co/Zr: 0.8, Cr/Zr: 0.8	Co/Cr: 0.9, Co/Zr: 1.0, Cr/Zr: 0.7
MZ	56	Co/Mo: 0.8, Co/Zr: 0.9, Mo/Zr: 0.8	Co/Mo: 0.9, Co/Zr: 1.1, Mo/Zr: 0.7
WZ	187	Co/W: 0.8, Co/Zr: 0.9, W/Zr: 0.8	Co/W: 0.9, Co/Zr: 1.1, W/Zr: 0.7

^aAverage from five points in SEM image.

BET values of WZ and CrZ powders are larger than the other catalysts. This indicates that addition of W and Cr is able to prevent particles agglomeration and thus increase the BET surface area of catalysts. This result is confirmed already by FE-SEM images, Figure 2. As seen, the surface area of Co-B10 is larger than Co-B60. This indicates that lower temperature prevent particle agglomeration and thus increase the BET surface area of catalysts. The Co, Cr, Mo, W and Zr contents of the catalysts were determined by ICP-OES and EDS. For ICP analysis, each powder dissolved in boiled aqua regia solution, HNO₃/HCl (1/3 ratio). More investigation was achieved by EDS pattern. Since EDS pattern shows only elemental analysis of one point of catalyst surface, it is not trustworthy. For this reason, five points of each catalyst surface were tested for Co, Cr, Mo, W and Zr contents. The average results are also shown in Table 1. It is found that EDS data is closed to ICP analysis.

Reduction of 4-NP to 4-AP

The catalytic activity of the synthesized catalysts was investigated for the reduction reaction of 4-NP to 4-AP in the presence of excess NaBH₄ in aqueous medium at room temperature (298 K). The reaction was monitored by using a UV-Vis spectroscopy. An aqueous solution of 4-nitrophenol exhibited the maximum absorption at 317 nm. The concentration of the NaBH₄ greatly exceeds those of 4-NP and the catalysis nanoparticles. The excess of NaBH₄ used increased the pH of the reacting system, but by that means retarded the degradation of BH₄⁻, and the liberated hydrogen purged out air, thereby checking the aerial oxidation of the reduced product of 4-NP. Furthermore, because the concentration of BH₄⁻ is very high, it remains essentially constant during the reaction. Upon addition of NaBH₄ to a 4-NP solution, the color rapidly changed from light to deep yellow. UV-Visible spectroscopy illustrated a red-shift in the absorption maximum from 317 nm for the 4-NP (solution pH = 5) starting material to 400 nm due to the generation of 4-nitrophenolate (solution pH = 7), Figure 3.

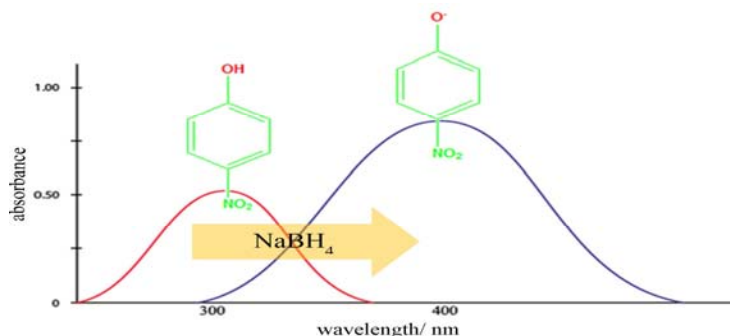


Figure 3. UV-Vis spectra of 4-NP solution before and after NaBH_4 addition.

The experiments in the presence and absence of the nano catalysts are performed under similar conditions. After addition of the catalyst, the color of 4-nitrophenolate started to fade with time. As seen in Figure 4, in the absence of catalyst, no decrease of the absorbance peak at 400 nm is observed, even after 60 days.

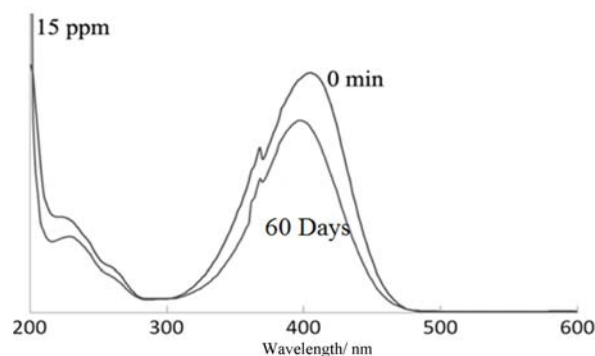


Figure 4. Reduction of 4-NP solution in the absence of catalysts.

This observation indicates that the reduction reaction was unable to occur by itself under the experimental conditions without the addition of catalysts. Catalytic efficient of obtained catalysts are studied by examination of initial concentration of 4-NP and NaBH_4 aqueous solution. The most of the previous reports were done at 4-NP concentration maximum at 30 ppm [32-38]. While in this work catalytic activity of obtained catalysts were tested on reduction of 4-NP initial concentration at ranges of 50-200 ppm. As seen later, it is found that our catalysts are highly active for high concentrations of 4-NP. Figure 5 shows time-dependent UV-Vis spectra of 4-NP reduction over Co-B10 nano catalyst.

For $[4\text{-NP}] = 50$ ppm, almost immediately after addition of Co-B10 to 4-NP/ NaBH_4 solution that peak around 400 nm attributed to 4-NP is disappeared and new peak around 300 nm is formed. It has generally been accepted that the absorbance band at 300 nm signifies the formation of 4-AP. Reduction of $[4\text{-NP}] = 100$ and 200 ppm are also shown in Figure 5. It is found that, required time for reduction reaction is increased by increasing initial concentration of 4-NP. Indeed, by increasing of initial concentration of 4-NP from 50 to 200 ppm reduction time is increased from 2 to 25 min. Catalytic activity results of Co-B60 amorphous nano catalyst are shown in Figure 6.

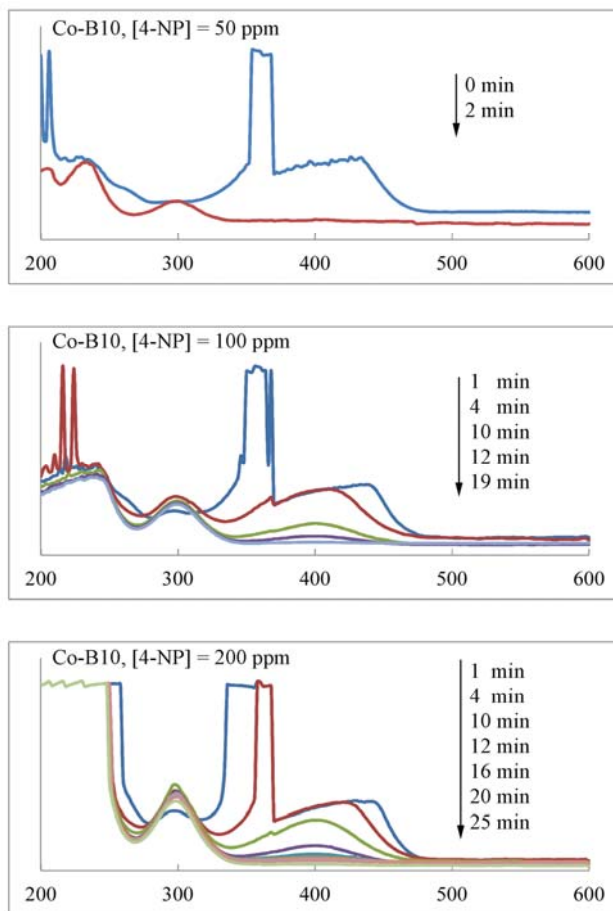


Figure 5. Time-dependent plots of reduction reaction at various concentration of 4-NP: Co-B10 = 6 mg, $[\text{NaBH}_4] = 0.3 \text{ M}$.

It can be seen that Co-B60 catalyst is weaker than Co-B10. It is probably attributed to the BET value of them. Because of larger surface area and subsequently more active site for hydrolysis of NaBH_4 solution by Co-B10 powder, it is faster, easier and significant reduction reaction. Figure 7 shows time-dependent UV-Vis spectra of 4-NP reduction over CrZ, MZ and WZ nano catalysts. For WZ at $[\text{4-NP}] = 50 \text{ ppm}$, after 12 min that peak around 400 nm attributed to 4-NP is disappeared and new peak around 300 nm is formed.

It can be seen that MZ nano catalyst needs higher time to reduce 4-NP. It is probably attributed to BET value of MZ. As already mentioned SEM image of MZ confirms many agglomerated particles. However, WZ is the best catalyst among the quaternary catalysts prepared in this work. Effect of NaBH_4 concentration on reduction reaction of 4-NP is studied. Figure 8 shows effect of two concentration of $[\text{NaBH}_4] = 0.15$ and 0.3 M on catalytic reduction of $[\text{4-NP}] = 25 \text{ ppm}$ over Co-B60 binary catalyst. As seen, even at $[\text{NaBH}_4] = 0.15 \text{ M}$ Co-B60 is able to reduce 4-NP to 4-AP.

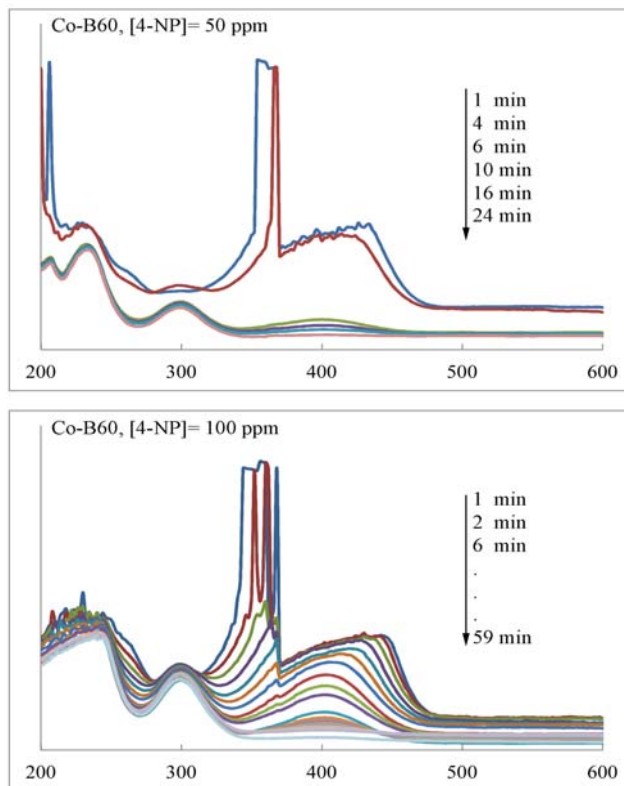


Figure 6. Time-dependent plots of reduction reaction at various concentration of 4-NP: Co-B60 = 6 mg, $[\text{NaBH}_4] = 0.3 \text{ M}$.

Figure 9 shows effect of NaBH_4 concentration on catalytic reduction of 4-NP over CrZ, MZ and WZ nano catalysts. It can be seen that, CrZ is not able to reduce 4-NP at low concentration of NaBH_4 while MZ nano catalyst converted 4-NP to 4-AP at 30 min. As seen, activity of MZ at $[\text{NaBH}_4] = 0.15$ and 0.3 M is almost similar.

According to the Langmuir-Hinshelwood model [39], BH_4^- should adsorb over electron-rich sites, such as O^\ominus or M^0 , which would transfer their electronic density towards the B element. H_2O should adsorb over electron-deficient sites, such as $\text{M}^{\delta+}$, which would attract the electronic density of O of H_2O . Then, one of the protonic H of H_2O interacts with one of the hydridic H of BH_4^- . This combination resulted in formation of H_2 gas evaluation. In the same time, 4-NP molecules were also adsorbed on the surface of the catalyst. These two steps were assumed to be reversible and modeled by Langmuir isotherm. It was also assumed that the diffusion of the reactants to the catalyst as well as all the adsorption/desorption equilibriums was fast. The reduction of 4-NP, which was the rate-determining step, took place by the reaction of adsorbed 4-NP with the surface-hydrogen species. After the reaction detachment of the product (4-AP) generated free surface and the catalytic cycle continued. No impurity peak is observed in the HPLC analysis of the products obtained in reduction reaction. The selective formation of 4-AP is further confirmed by FT-IR and NMR spectroscopic analysis. FT-IR data: ν (cm^{-1}): 3179 (OH), 3338 and 3277 (NH_2), 3031 (aromatic C-H), 1612 (aromatic C=C). ^1H NMR data DMSO- d_6 , Δ (ppm): 8.34 (s, 1H, -OH); 6.50 (d, 2H, ArH); 6.40 (d, 2H, ArH),

4.80 (s, 2H, NH₂). The amorphous nano catalysts were separated from the reaction mixtures by filtration after the reduction reaction and the filtrates were used for determination of metal ions leaching by ICP emission spectroscopy. No ion was detected in the filtrate. We speculated the proposed mechanism as showed in Scheme 1.

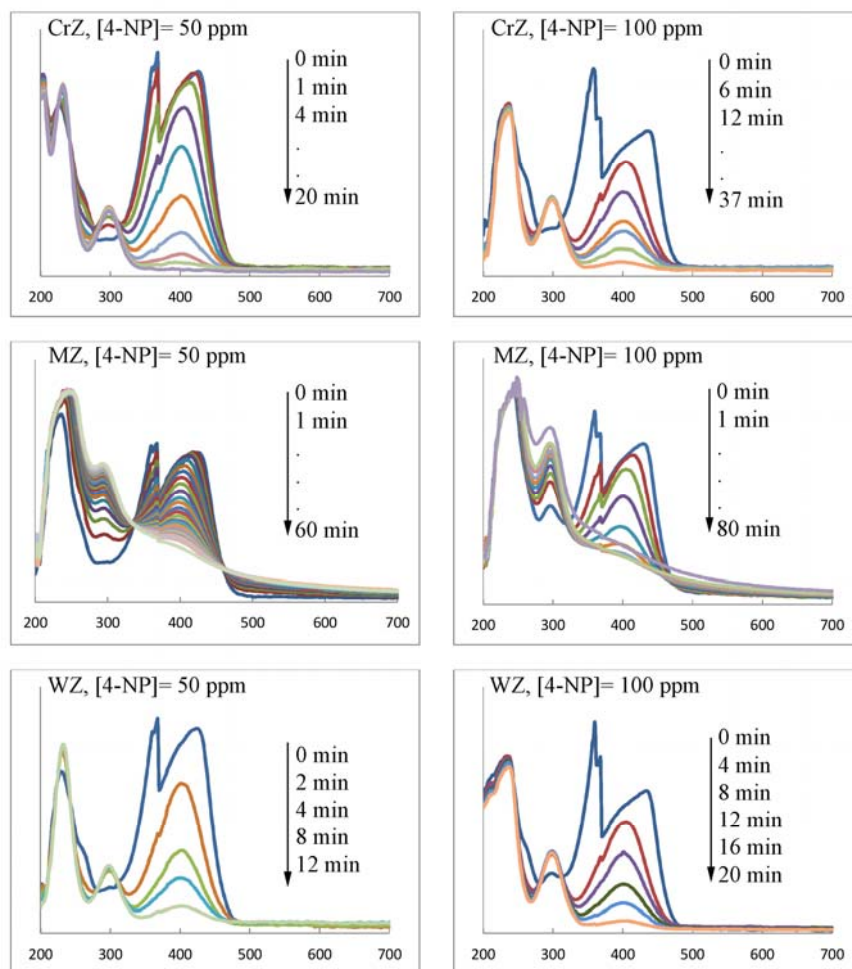


Figure 7. Time-dependent plots of reduction reaction at various concentration of 4-NP: catalyst = 6 mg, [NaBH₄] = 0.3 M.

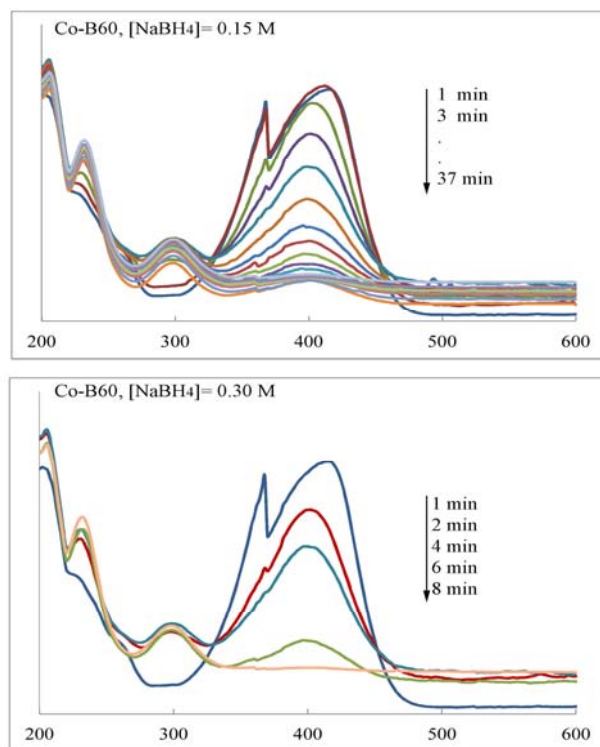
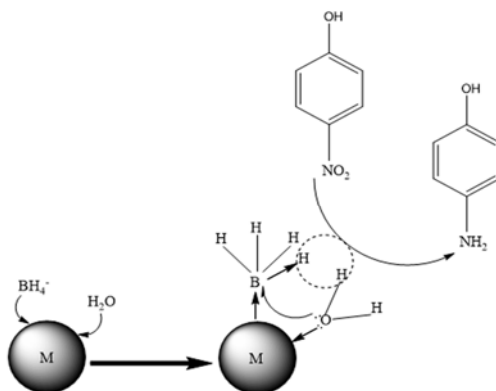


Figure 8. Effect of NaBH_4 concentration on reduction of $[4\text{-NP}] = 25$ ppm over Co-B60.



Scheme 1. Proposed mechanism for reduction of 4-NP.

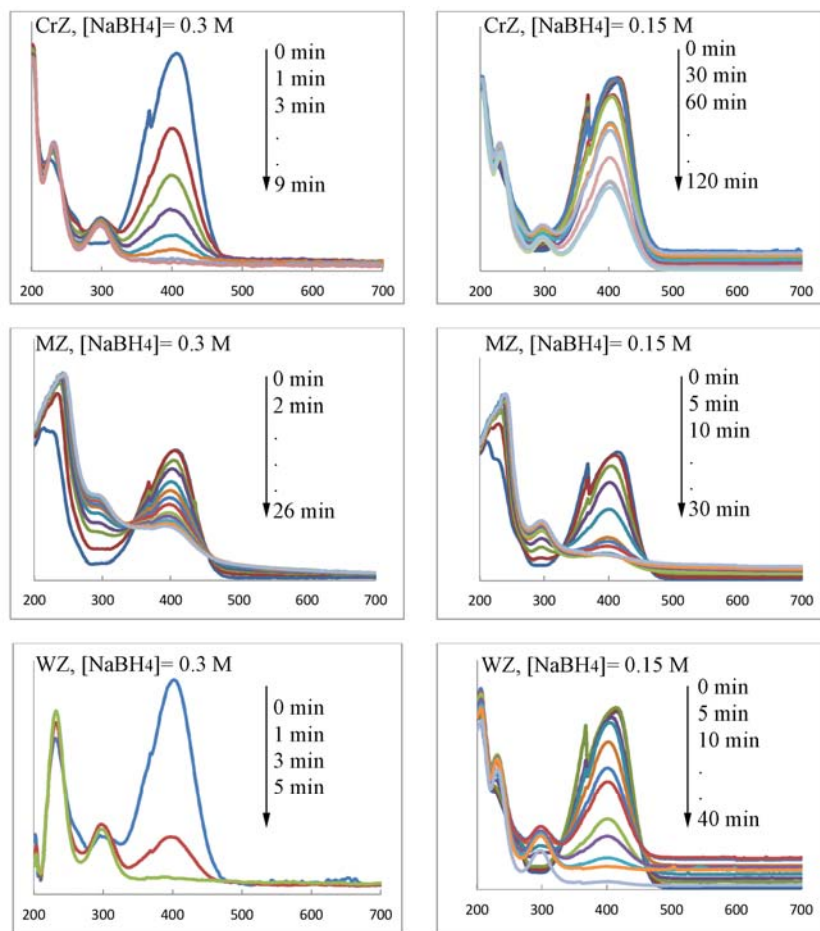


Figure 9. Effect of NaBH_4 concentration on reduction of [4-NP] = 25 ppm.

CONCLUSIONS

In summary, our study on the preparation, characterization and application of binary and quaternary amorphous nano catalysts led to the following conclusions: Amorphous nano catalysts were synthesized by ultrasound-assisted method. Effect of preparation temperature on size, morphology and catalytic activity of Co-B amorphous nano catalysts was studied. Indeed, effect of preparation temperature on size, morphology and consequently catalytic activity of Co-B amorphous nano catalysts were studied. Co-M-Zr-B (M: Cr, Mo and W) as quaternary catalysts are also prepared by same method. Catalytic activity of synthesized catalysts are tested on reduction of 4-NP to 4-AP under UV-Vis monitoring. XRD patterns indicating that all five catalysts possessed amorphous phase. BET order of prepared catalysts can be ranked $\text{WZ} > \text{CrZ} > \text{CoB10} > \text{CoB60} > \text{MZ}$. This order almost can be ranked for catalytic activity through reduction of 4-NP to 4-AP.

ACKNOWLEDGMENTS

The authors are grateful to the Research Council of University of Guilan for the partial support of this study.

REFERENCES

- Schrinner, M.; Ballauff, M.; Talmon, Y.; Kauffmann, Y.; Thun, J.; Möller, M.; Breu, J. *Science* **2009**, 323, 617.
- Nolte, P.; Stierle, A.; Jin-Phillipp, N.Y.; Kasper, N.; Schulli, T.U.; Dosch, H. *Science* **2008**, 321, 1654.
- Tian, N.; Zhou, Z.Y.; Sun, S.G.; Ding, Y.; Wang, Z.L. *Science* **2007**, 316, 732.
- Weddle, K.S.; Aiken III, J.D.; Finke, R.G. *J. Am. Chem. Soc.* **1998**, 120, 5653.
- Telkar, M.M.; Rodea, C.V.; Chaudhari, R.V.; Joshi, S.S.; Nalawade, A.M. *Appl. Catal. A: Gen.* **2004**, 273, 11.
- Yu, D.; Yam, V.W. *J. Phys. Chem. B* **2005**, 109, 5497.
- Rashid, M.H.; Mandal, T.K. *J. Phys. Chem. C* **2007**, 111, 16750.
- Feng, Y.; Yin, H.; Gao, D.; Wang, A.; Shen, L.; Meng, M. *J. Catalysis* **2014**, 316, 67.
- Feng, Y.; Yin, H.; Wang, A.; Gao, D.; Zhu, X.; Shen, L.; Meng, M. *Appl. Catal. A: Gen.* **2014**, 482, 49.
- Wang, A.; Yin, H.; Lu, H.; Xue, J.; Ren, M.; Jiang, T. *Langmuir* **2009**, 25, 12736.
- Uken, A.H.; Bartholomew, C.H. *J. Catal.* **1980**, 65, 402.
- Li, H.; Wu, Y.; Luo, H.; Wang, M.; Xu, Y. *J. Catal.* **2003**, 214, 15.
- Li, H.; Li, H.; Dai, W. L.; Qiao, M.H. *Appl. Catal. A Gen.* **2003**, 238, 119.
- Li, H.X.; Li, H.; Wang, M. *Appl. Catal. A Gen.* **2001**, 207, 129.
- Lu, D. S.; Li, W.S.; Jiang, X.; Tan, C.L.; Zeng, R.H. *J. Alloy Compd.* **2009**, 485, 621.
- Shen, J.; Li, Z.; Yan, Q.; Chen, Y. *J. Phys. Chem.* **1993**, 97, 8504.
- Li, H.; Luo, H.; Zhuang, L.; Dai, W.; Qiao, M. *J. Mol. Catal. A Chem.* **2003**, 203, 267.
- Esumi, K.; Isono, R.; Yoshimura, T. *Langmuir* **2004**, 20, 237.
- Du, Y.; Chen, H.L.; Chen, R.Z.; Xu, N.P. *Appl. Catal. A: Gen.* **2004**, 277, 259.
- Vaidya, M.J.; Kulkarni, S.M.; Chaudhari, R.V. *Org. Process Res. Dev.* **2003**, 7, 202.
- Yoo, B.W.; Kim, D.; Kim, H.M.; Kang, S.H. *Bull. Korean Chem. Soc.* **2012**, 33, 2851.
- Duan, Z.; Ma, G.; Zhang, W. *Bull. Korean Chem. Soc.* **2012**, 33, 4003.
- Naik, B.; Hazra, S.; Prasad, V.S.; Ghosh, N.N. *Catal. Commun.* **2011**, 12, 1104.
- Kuroda, K.; Ishida, T.; Haruta, M. *J. Mol. Catal. A: Chem.* **2009**, 298, 7.
- Naik, B.; Hazra, S.; Muktesh, P.; Prasad, V.S.; Ghosh, N.N. *Sci. Adv. Mater.* **2011**, 3, 1025.
- Shojaei, A.F.; Rafie, M.D.; Loghmani, M.H. *Bull. Korean Chem. Soc.* **2012**, 33, 2748.
- Shojaei, A.F.; Loghmani, M.H. *Bull. Korean Chem. Soc.* **2012**, 33, 3981.
- Shojaei, A.F.; Tabari, A.R.; Loghmani, M.H. *Micro Nano Lett.* **2013**, 8, 426.
- Loghmani, M.H.; Shojaei, A.F. *J. Alloys Compd.* **2013**, 580, 61.
- Loghmani, M.H.; Shojaei, A.F. *Int. J. Hydrogen Energy* **2013**, 38, 10470.
- Loghmani M.H.; Shojaei, A.F. *Energy* **2013**, 68, 152.
- Kuroda, K.; Ishida, T.; Haruta, M. *J. Mol. Catal. A: Chem.* **2009**, 298, 7.
- Naik, B.; Prasad, V.S.; Ghosh, N.N. *Powder Technology* **2012**, 232, 1.
- Mandlimath, T.R.; Gopal, B. *J. Mol. Catal. A: Chem.* **2011**, 350, 9.
- Tang, S.; Vongehr, S.; Zheng, Z.; Meng, X. *J. Colloid Interface Sci.* **2010**, 351, 217.
- Hallett-Tapley, G.L.; Crites, C.-O.L.; González-Béjara, M.; McGilvray, K.L.; Netto-Ferreira, J.C.; Scaiano, J.C. *J. Photochem. Photobiol. A* **2011**, 224, 8.
- Zhang, W.; Tan, F.; Wang, W.; Qiu, X.; Qiao, X.; Chen, J. *J. Hazard. Mater.* **2012**, 217, 36.
- Murugan, E.; Jebaranjitham, J.N. *J. Mol. Catal. A: Chem.* **2012**, 365, 128.
- Wunder, S.; Polzer, F.; Lu, Y.; Mei, Y.; Ballauff, M. *J. Phys. Chem. C* **2010**, 114, 8814.